Avicenna Journal of Phytomedicine (AJP)

Original Research Article

Green synthesis of silver-coated zinc oxide nanocomposite using the walnut green husk extract and assessment of its cytotoxicity and antimicrobial activity against *Streptococcus mutans*

Hossein Nematollahi[1], Taraneh Movahhed[1], Majid Darroudi[2], Hasan Rakhshandeh[3], Hadi Farsiani[4], Alieh Charmeh[1,*]

[1]*Department of Pediatric Dentistry, School of Dentistry, Mashhad University of Medical Sciences, Mashhad, Iran*
[2]*Department of Modern Science and Technology, Mashhad University of Medical Sciences, Mashhad, Iran*
[3]*Department of Pharmacology, Pharmacological Research Center of Medicinal Plants, School of Medicine, Mashhad University of Medical Sciences, Mashhad, Iran*
[4]*Department of Microbiology and Virology, Antimicrobial Resistance Research Center, School of Medicine, Mashhad University of Medical Sciences, Mashhad, Iran*

Article history:
Received: Oct 18, 2022
Received in revised form: Oct 07, 2023
Accepted: Feb 26, 2024
Epub ahead of print

**** Corresponding Author:***
Tel: +98-9158638060
Fax: +98-5632445040
charmeh.1370@gmail.com

Keywords:
Dental caries
Streptococcus mutans
Zinc oxide
Nanocomposites
Green synthesis
Green husk

Abstract

Objective: This study aimed to synthesize and characterize silver-coated zinc-oxide (ZnO/Ag) nanocomposite using green husk extract of Persian Walnut (*Juglans regia L.*) and evaluate its cytotoxicity and antimicrobial activity against Streptococcus *mutans*.

Materials and Methods: In this *in vitro* experimental study, five groups were tested: hydroethanolic green husk extract (group A), green-synthesized ZnO/Ag nanocomposite using the extract (group B), chemically synthesized ZnO/Ag nanocomposite (group C), 0.2% chlorhexidine (positive control), and distilled water (negative control). Antibacterial activity against *S. mutans* was assessed via agar-well diffusion (inhibition zone diameters) and broth microdilution (MIC and MBC). Cytotoxicity was evaluated using the MTT assay. Tests were performed in triplicate across serial dilutions, with data analyzed by ANOVA.

Results: Group A exhibited no inhibitory or bactericidal effect on *S. mutans*. Group B inhibited growth at 125 ppm, and group C at 31.25 ppm. Both groups B and C reduced *S. mutans* colony counts by approximately 3 logs (significant vs. group A) and showed minimal cytotoxicity.

Conclusion: Both green-synthesized and chemically synthesized ZnO/Ag nanocomposites displayed lower antibacterial activity than chlorhexidine (CHX) against *S. mutans*, along with lower cytotoxicity, yet achieved a significant reduction in bacterial colony count.

Please cite this paper as:
Nematollahi H, Movahhed T, Darroudi M, Rakhshandeh H, Farsiani H, Charmeh A. Green synthesis of silver-coated Zinc Oxide nanocomposite using the walnut green husk extract and assessment of its cytotoxicity and antimicrobial activity against Streptococcus mutans. Avicenna J Phytomed, 2024. Epub ahead of print.

Introduction

Several strategies have been employed to control dental caries. Antimicrobial agents such as chlorhexidine (CHX), artificial sweeteners such as xylitol, and remineralizing agents such as fluoride have been used in different forms of toothpaste, mouthwash, gel, varnish, and restorative materials aiming to control dental caries. Although all these products have been successful in decreasing the *Streptococcus mutans* (*S. mutans*) count, evidence shows that the bacterial count reaches its baseline value a couple of weeks to months after using these products. Thus, these products should be regularly used to have long-term effects (Li and Tanner 2015).

Mechanical plaque control by use of a toothbrush and dental floss is the main strategy for dental plaque removal. Mouthwashes are used as an adjunct for supragingival plaque control and prevention of gingivitis (Azizi et al. 2008). CHX mouthwash is the gold-standard antimicrobial mouthwash with optimal properties such as prevention of smooth-surface caries, control of gingival inflammation, and reduction of microbial plaque (James et al. 2017; Pandiyan et al. 2022; Poppolo Deus and Ouanounou 2022). However, it has several drawbacks such as tooth discoloration, alteration of the sense of taste, xerostomia and oral mucosal burning sensation that limit its long-term application (Balagopal and Arjunkumar 2013; Polizzi et al. 2020; Poppolo Deus and Ouanounou 2022). Thus, researchers are in search of an alternative with optimal antimicrobial activity and minimal complications. An ideal mouthwash should be non-allergic, must have optimal anti-plaque and antibacterial properties, favorable taste and odor, and minimal cytotoxicity, and should not cause tooth discoloration or adversely change the microbial oral flora (Golfeshan et al. 2020; Iskandar et al. 2022; Rajendiran et al. 2021; Waqar et al. 2022).

Considering the recently decreased interest of patients in chemical medications, herbal products have gained increasing popularity (Philip et al. 2019). According to a report by the World Health Organization, over 80% of the population of developing countries believe in the optimal efficacy of medicinal plants, and use them for the treatment of common diseases (Ameh et al. 2010; Mazzari and Prieto 2014; Oliveira et al. 2012).

Nuts, particularly walnuts, are the main source of phenolic compounds with high antioxidant activity (Moosavi Dolatabadi et al. 2015; Safarian et al. 2016). Persian Walnut (*Juglans regia L.)* has the highest level of antioxidants (Mishra et al. 2010). Juglone is the most widely recognized phenolic compound in walnut green husks (Jaimand et al. 2004), which can inhibit the key enzymes in bacterial metabolism (Jahanban-Esfahlan et al. 2017). The cariostatic effect of walnut green husk has also been reported (Khattak et al. 2022).

Metal nanoparticles have long been used in medicine and dentistry due to their bactericidal and bacteriostatic properties (AbdElRahman et al. 2002; Bandow et al. 2003; Mozaffari et al. 2005). Decreasing the size of metal particles from micro-scale to nano-scale (< 100 nm) increases their contact area and subsequently, their efficacy (Holister et al. 2003). Zinc oxide (ZnO) nanoparticles are extensively used in dentistry for caries control. The safety of ZnO nanoparticles has also been confirmed by the Food and Drug Administration (Jin et al. 2009). Silver (Ag) nanoparticles also have high antibacterial activity; however, they cannot be extensively used as a therapeutic agent due to their considerable cytotoxicity (Wang et al. 2017). Silver-coated zinc oxide (ZnO/Ag) nanocomposite has low cytotoxicity and considerable antibacterial activity and can eliminate the bacteria by degrading their cell membrane (Azizi et al. 2016; Lu et al. 2017; Wang et al. 2017).

Considering the role of *S. mutans* as the main culprit responsible for the development of dental caries, and the recent popularity of the green synthesis method,

this study aimed to synthesize and characterize ZnO/Ag nanocomposite using the walnut green husks extract and assess its cytotoxicity and antimicrobial activity against *S. mutans*.

Materials and Methods

This *in vitro* experimental study was conducted on standard strain *S. mutans* (ATCC 25175) obtained from the Pasteur Institute of Iran. The antibacterial properties of ZnO/Ag nanocomposite, CHX, and distilled water against *S. mutans* and the cytotoxicity of the materials was evaluated against the Hela cell line using 96 samples.

Preparation of the hydroalcoholic extract of green husk and stock solution of the materials

The green husks of Persian walnut, with the scientific name *Juglans regia L.* (*J. regia L.*), was collected from Khorasan Razavi Province and its identity was confirmed in the herbarium of Ferdowsi University, Mashhad, Iran. Dried green husk was placed in an extraction heater (Electromantle, UK) and the obtained extract was concentrated in a rotary device. To quantitatively analyze the phenolic compounds, the Folin–Ciocâlteu reagent was used; 20 µl of the extract (10 mg/ml) was mixed with 100 µl of Folin–Ciocâlteu reagent and 30 µl of 1 mol/L sodium bicarbonate, and the volume of the mixture reached 2 ml using deionized water. After 2 hr, the optical density of the mixture was measured by a spectrophotometer at 765 nm wavelength. To draw the calibration curve, gallic acid was used. Gallic acid at the levels of 50 to 500 mg/ml was mixed with 100 µl Folin–Ciocâlteu reagent and 30 µl of 1 mol/L sodium bicarbonate, and the optical density of the solution was read, and the calibration curve was drawn. The total phenolic content of the extract was calculated corresponding to the amount of gallic acid (mg) per gram of dry extract using the gallic acid standard curve. The total phenolic content of the green husk extract was found to be 46.7 mg (Hosseini et al. 2017).

The solvent was evaporated at low pressure using a solvent evaporator device. The concentrated extract was kept refrigerated. For the tests, 0.5 g of the green husk extract was dissolved in 1 ml of distilled water.

Green synthesis of ZnO/Ag nanocomposite using the green husk hydroethanolic extract

First, 7.43 g Zn $(NO_3)_2$. $6H_2O$ was dissolved in 50 ml of distilled water and then, 150 ml of the green husk hydroethanolic extract was added in a dropwise manner. The solution was stirred at room temperature for 1 hr. Next, 20 ml of 0.05 M dodecyl sulfate was added as surfactant, and the mixture was stirred for 30 min at room temperature. Next, 20 ml 3% silver nitrate was added, which changed the color of the mixture to black, indicating the formation of silver nanoparticles on the surface of ZnO in a sol solution. Next, the sol solution was placed in a paraffin bath at 80°C for 12 hr, and stirred by a magnetic stirrer operating at 700 rpm. After 12 hr, the water was evaporated and a sticky gel remained at the bottom of the plate. The obtained gel was placed in an oven at 100°C for 6 hr to dry. The well-grounded dried gel in a mortar and pestle (oily), divided into five portions (Ghazal et al. 2020; Ghazal et al. 2021; Maleki et al. 2021). One portion was used for the thermogravimetric analysis/differential thermal analysis (TGA/DTA), and the remaining four portions were placed in an oven for 2 hr at 400, 500, 600, and 700°C for calcination. Finally, a brown powder, which was ZnO/Ag nanocomposite was obtained. The nanocomposite synthesized by the green method underwent TGA/DTA, Fourier-Transform infrared spectroscopy (FTIR), UV-Vis, X-ray diffraction (XRD), field emission scanning electron microscopy (FE-SEM), and energy-dispersive X-ray spectroscopy (EDX) for characterization.

Bacterial culture

Standard strain *S. mutans* (ATCC 25175) was obtained from the microbial bank of the Pasteur Institute of Iran, and incubated in Mueller Hinton blood agar for 24 hr in an anaerobic jar containing CO_2 using a Gas-Pak at 37°C. The turbidity of the suspension was set at 0.5 McFarland (containing 15×10^6 bacteria) by using a spectrophotometer (Eppendorf, Germany).

Assessment of antibacterial activity of the materials

Both agar-well diffusion and broth microdilution methods were used for this purpose. In both methods, 0.2% CHX (2 mg/ml) served as the positive control and distilled water served as the negative control. Each test was repeated in triplicate.

The following groups were studied: Group A: Hydroethanolic extract of green husk. Group B: ZnO-Ag nanocomposite synthesized by the green method using green husk hydroethanolic extract. Group C: ZnO-Ag nanocomposite alone. Group D: CHX. Group E: Distilled water.

Agar-well diffusion

After preparation of the microbial suspension with 0.5 McFarland standard concentration, it was streak-cultured on Mueller Hinton blood agar by a sterile swab. Ten serial dilutions of groups A, B and C were prepared starting from a concentration of 500 ppm. Ten dilutions were prepared from each material. Next, the tip of a 5-mm sterile tube was used to create wells in the culture medium corresponding to the number of prepared dilutions; 30 µl of each dilution was added to each well. The plates were then incubated in an anaerobic jar containing CO_2 at 37°C. The diameter of the growth inhibition zones was measured by a ruler in millimeters (mm).

Broth micro-dilution

A sterile 96-well plate was used for this method. After preparing 0.5 McFarland standard suspension of *S. mutans*, 100 µl of Mueller Hinton broth was added to 10 wells; 100 µl of the extract was then added to the first well. Next, 100 µl of the contents of the first well was transferred to the second well. After homogenization, 100 µl of the obtained mixture was transferred to the third well. This process was repeated until the 10^{th} well; eventually, 100 µl of the 10^{th} well was discarded. Accordingly, 8 serial dilutions were prepared from each of the A, B and C groups. Finally, 5 µl of bacterial suspension (1×10^6 concentration) was added to the 1^{st} to the 9^{th} wells. The number of bacteria in each well was approximately 5×10^4. The 9^{th} (containing bacteria and broth medium) and the 10^{th} (containing broth medium alone) wells served as the positive and negative controls, respectively, for bacterial proliferation.

Broth macro-dilution

This technique was used for the assessment of the green husk hydroethanolic extract alone. Ten test tubes were used in this technique; 0.5 ml of the broth was added to each test tube. Next, 0.5 ml of the extract was added to the 1^{st} test tube, and after homogenization, 0.5 ml of the contents of the 1^{st} tube was transferred to the second tube. This process was repeated until the 8^{th} tube; 0.5 ml of the 8^{th} tube was discarded. Next, 0.5 ml of *S. mutans* suspension (1×10^6 bacteria) was added to all test tubes (except for the 10^{th} tube). Accordingly, the bacterial concentration in each tube was 5×10^5 bacteria. The 9^{th} (containing bacteria and broth) and 10^{th} (containing broth alone) test tubes were used as the positive and negative controls, respectively, for bacterial proliferation.

Assessment of cytotoxicity

The methyl thiazolyl tetrazolium (MTT) assay was used for this purpose, along with the Hela cancer cell line obtained from the cell bank of the Pasteur Institute of Iran. The cell culture flask was evaluated for possible contamination after reaching 80% confluence. The medium was clear and microscopic assessment revealed

multi-dimensional cells with no fungal hyphae. The cell culture flask was rinsed with phosphate-buffered saline twice. Then, trypsin was added to cover the cells, and epithelial cells were incubated at 37°C for 3 min. After inspection under an inverted microscope and observing the round shape of cells, trypsin was removed and the flask was slightly shaken to detach the cells; 5 ml of the cell culture medium was added to the flask and the Hela cell suspension was transferred into a Falcon tube and centrifuged at 1500 rpm for 4 min. The supernatant was discarded and 1 ml of the cell culture medium was added. The cells were then counted using Trypan blue and a Neubauer chamber. Thirty cell culture well plates were required for each extract, each with three repetitions (considering eight serial dilutions of each of the four groups as well as the control and blank wells). The total number of cells was calculated using the following formula:

Total cell count = Cell counter total× Volume of cell suspension× Reverse dilution× 10^4

Accordingly, the number of cells in each well was calculated as follows:

Total cells × X=total medium of plate× total cell of plate

A total of 1 ×10^4 cells were considered for each well; each well was filled with 100 µl of the culture medium. The cell culture plate was incubated at 37°C for 24 hr. After the incubation period of the cell culture plate, serial dilutions of the study groups were prepared. 500 µl of DMEM cell culture medium with 5% FBS was poured into seven sterile 1.5-ml microtubes. 500 µl of the extract, which was available as a solution, was added to the microtube and after homogenizing the solution, 500 µl of it was added to the next tube and this process continued until the final dilution.

500 µl of the extract solution was added to the first microtube and after mixing, 500 µl of it was transferred to the next tube and so on. After controlling the cell status, the overlaying medium was discarded and the cell culture plate was rinsed with phosphate-buffered saline twice; 100 µl of each microtube content was added to each three-well column (for three repetitions) and two columns of the plate served as the control wells without extract and blank wells without cells and extract. After the addition of extract, the cell culture plate was incubated at 37°C for 20 hr; 0.001 g of the MTT powder was dissolved in 1 mL of the culture medium; the volume reached 10 ml; 1 ml of the content reached 10 ml volume again. After discarding the culture medium of the well, the cell culture plate was gently rinsed with phosphate-buffered saline (to prevent detachment of cells from the plate). Next, 100 µl of the MTT solution was added to each well and incubated at 37°C for 4 hr; 100 µl of dimethyl sulfoxide was added to each well. The plate was covered with aluminium foil and placed on an orbital shaker operating at 70 rpm at room temperature for 10 min. The optical density of the plate wells was then read at 570 to 630 nm wavelength using a spectrophotometer (Eppendorf, Germany).

IC_{50}: IC_{50} of groups A-C was calculated by the CalcuSyn software using the mean optical density values. IC_{50} refers to the concentration of material that inhibits the viability of cells by 50%, and was calculated using the following formula:

Cell viability (%) = Mean OD^2/Control OD x 100%

The cell viability for A, B, C, and D extracts was 0.95, 0.95, 0.90, and 0.90, respectively, indicating the accuracy of the test.

Statistical analysis

The normal distribution of data was evaluated by the Kolmogorov-Smirnov test. Two-way ANOVA was used for pairwise comparisons of the mean values. One-way ANOVA and Tukey's test were applied for comparison with the negative and positive control groups.

Results

Characterization of ZnO/Age nanocomposite synthesized by the green method using the walnut green husk extract

The formation of this nanocomposite was confirmed by XRD, TGA/DTA, UV-vis, FTIR, FE-SEM, and EDX.

FTIR: To analyze the chemical structure and bonds of ZnO/Ag nanocomposite synthesized by the green method using the green husk extract, the FTIR spectra were obtained in the range of 400-4000 cm^{-1}. Figure 1 shows the infrared spectra of nanocomposite at 400, 500, 600 and 700°C. The stretching vibration of OH in the water molecule (with hydrogen bonds) at all four temperatures was noted as a strong band at 3452 cm^{-1}; this peak may be due to water sorption by the nanocomposite. A bending vibration belonging to the water molecule was noted at 1439 cm^{-1} which was the same at all four temperatures. Vibrations at 400-454 cm^{-1} were attributed to stretching vibrations of ZnO/Ag.

UV-Vis: The absorbance spectra of ZnO/Ag nanocomposite synthesized by the green method using the green husk extract at 400, 500, 600 and 700°C temperatures are presented in Figure 2.

A wide absorbance band was noted at 380 nm at 400°C, 379 nm at 500°C, 379 nm at 600°C, and 381 nm at 700°C. These peaks can be attributed to ligand metal charge transfer.

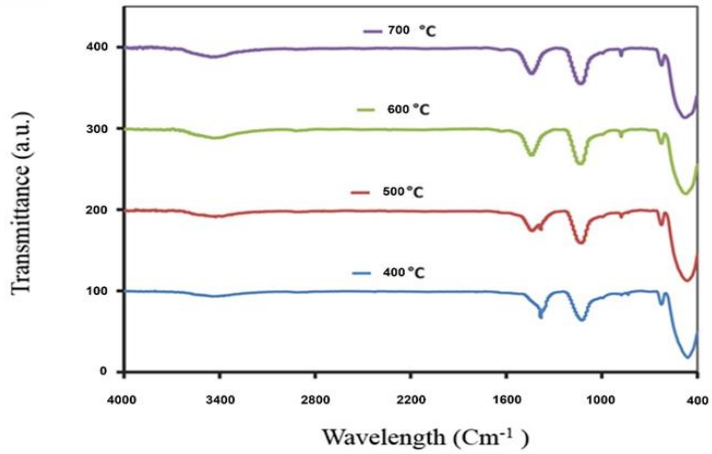

Figure 1. FTIR spectra of ZnO/Ag nanocomposite synthesized by the green method using the green husk extract at 400, 500, 600 and 700°C temperatures

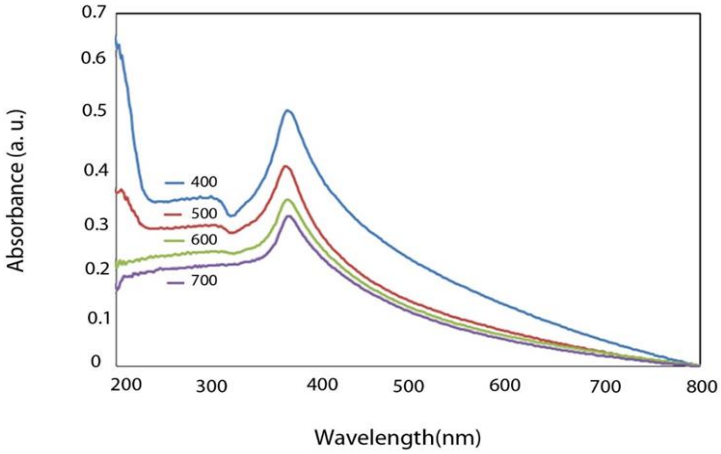

Figure 2. Absorbance spectra of ZnO/Ag nanocomposite synthesized by the green method using the green husk extract at 400, 500, 600 and 700 °C temperatures.

XRD: The XRD spectra of ZnO/Ag nanocomposite synthesized by the green method using the green husk extract at 400, 500, 600 and 700°C temperatures are presented in Figure 3. As shown, ZnO nanoparticles had a hexagonal network with diffraction peaks at 31.79, 34.48, 36.28, 47.56, 56.68, 62.88, and 67.96 Θ2 which represented Θ2100, 002, 101, 102, 110, 103, and 112, respectively according to the JCPDS-80-74 card. The peaks belonging to Ag showed a cubic centered network. The silver diffraction peaks at 38.12, 44.32 and 64.52 Θ2 represented 111, 200, and 220, respectively according to the JCPDS-82-0718 card. Sharp peaks in the spectra indicated a high degree of crystallinity. The size of particles was calculated according to Scherrer's equation and is reported in Table 1.

Table 1. Data obtained from the XRD regarding the size of the nanoparticles

Size (nm)	FWHM (rad.)	2Θ (deg.)	Temperature (°C)
46.2	0.004	38.72	400
46.2	0.004	38.80	500
34.65	0.004	38.64	600
46.2	0.004	38.80	700

FWHM: Full width at half maximum

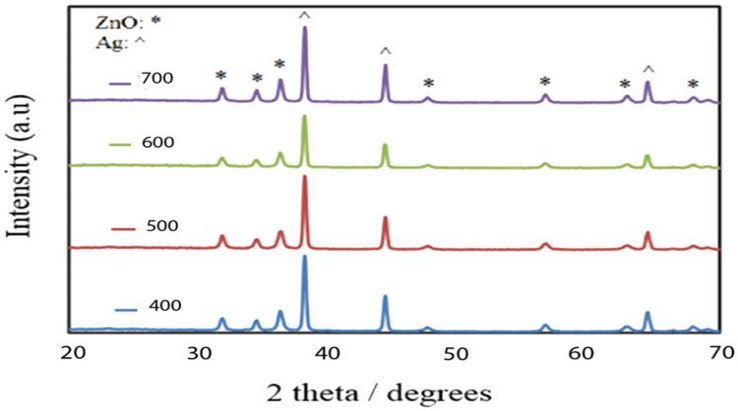

Figure 3. XRD spectra of ZnO/Ag nanocomposite synthesized by the green method using the green husk extract at 400, 500, 600 and 700°C temperatures.

TGA/DTA: The TGA/DTA spectra of ZnO/Ag nanocomposite synthesized by the green method using the green husk extract at 400, 500, 600 and 700°C temperatures are presented in Figure 4. As shown, the respective nanocomposite lost weight in an endothermic reaction and eventually, lost 66% of its weight in the process of heating. This weight loss occurred at 265°C due to the evaporation of water molecules and the formation of pure phases of ZnO/Ag. However, no further weight loss occurred at temperatures higher than 500°C, indicating the formation of nanocomposite as the end product.

FESEM/TEM/PSA/EDX: Figures 5 and 6 (a and b) shows FE-SEM and TEM micrographs of ZnO/Ag nanocomposite synthesized by the green method using the green husk extract at 500°C. As shown, nanoparticles had a relatively uniform growth and similar spherical morphology and average size of about 37.8 nm (Figure 6b). The EDX results regarding the elemental composition of ZnO/Ag nanoparticles are presented in Figure 7. According to the results, the synthesized nanocomposite was composed of oxygen, zinc and silver (Table 2).

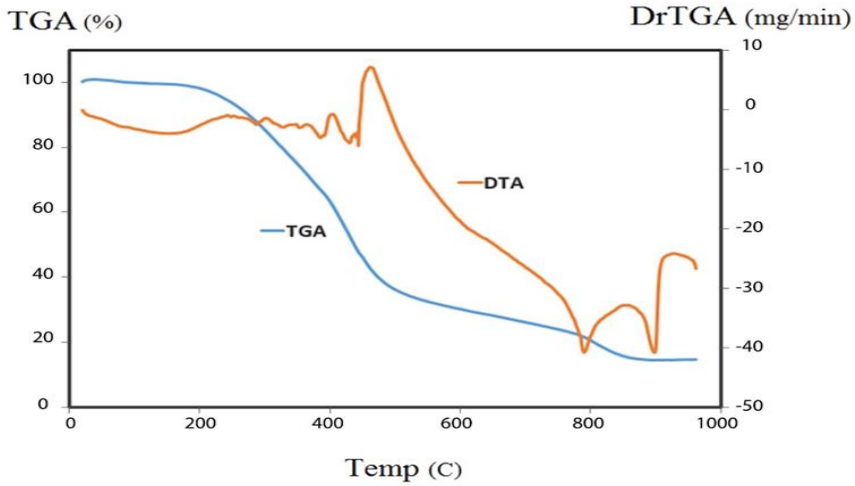

Figure 4. TGA/DTA spectra of ZnO/Ag nanocomposite synthesized by the green method using the green husk extract at 400, 500, 600 and 700°C temperatures; DrTGA: Derivative Thermogravimetric Analysis

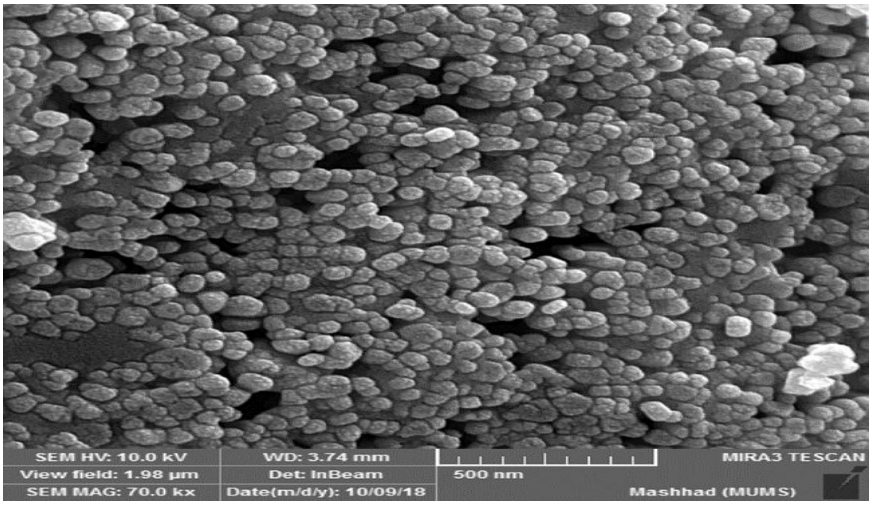

Figure 5. FE-SEM micrograph of the synthesized ZnO/Ag nanocomposite.

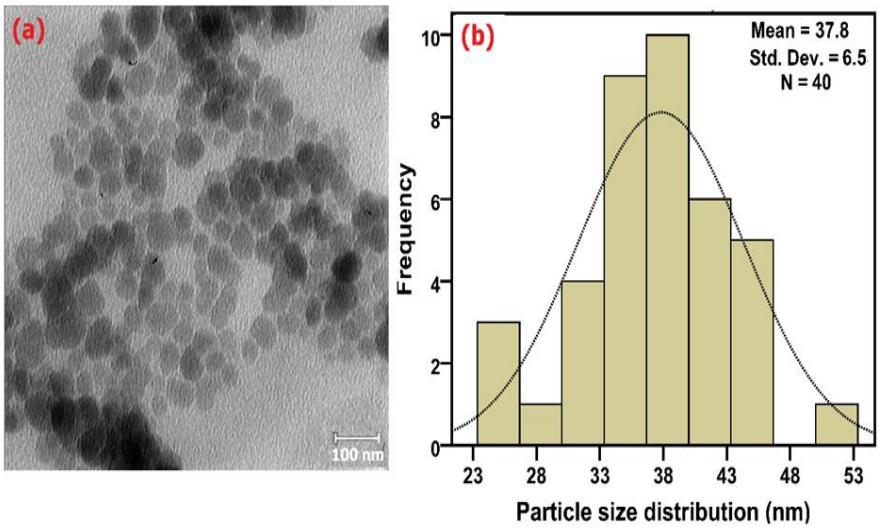

Figure 6. TEM micrograph (a) and PSA (b) of the synthesized ZnO/Ag nanocomposite.

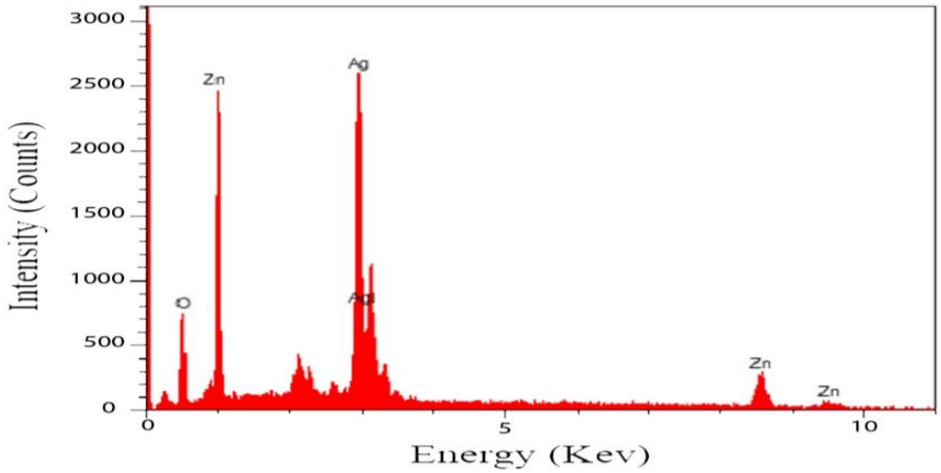

Figure 7. EDX results of ZnO/Ag nanocomposite synthesized by the green method using the green husk extract at 500°C temperature.

Table 2. EDX results regarding the synthesized nanocomposite

Element	*W%	*A%
O	30.54	72.19
Zn	15.17	8.78
Ag	54.29	19.04
Total	100	100

*A%: Atomic percentage; W%: Weight percentage

Antibacterial activity of the study groups

In agar diffusion test, *S. mutans* proliferated in all three groups of A, B, and C, and no growth inhibition zone formed in these three groups. The growth inhibition zone was not seen in the negative control group (distilled water) either.

Concerning broth micro-dilution test, Table 3 and Figures 8 and 9 present the results for the three repetitions of this test for groups A-C. As shown, group A (green husk extract alone) had no inhibitory or bactericidal effect on *S. mutans*. Group B (ZnO/Ag nanocomposite plus green husk extract) showed an MIC of 125 ppm. This concentration caused a 3 log reduction (1000 bacteria) in *S. mutans* count in the blood agar culture medium. Group C (nanocomposite alone) showed an MIC of 31.25 ppm with no bactericidal effect at this concentration on agar culture medium; however, *S. mutans* colony count decreased by a minimum of 3 log, which was considerable. The MIC and MBC of CHX were both 0.3 mg/ml (Figures 8 and 9).

Cytotoxicity

The first two concentrations of ZnO/Ag nanocomposite synthesized by the green method using the green husk extract showed maximum cytotoxicity and minimum optical density. In all groups, minimum optical density belonged to blank.

Figure 8. Bacterial growth in 8 dilutions transferred from the plate related to the different extract of the aqueous alcoholic extract of walnut green husk

.

Table 3. Results of broth micro-dilution test for groups A-C

Group	Concentration (ppm)	Culture medium color	Growth/no growth of bacteria
A: Green husk hydroalcoholic extract	500	Colorless/pink	Bacterial growth
	250	Colorless/pink	Bacterial growth
	125	Colorless/pink	Bacterial growth
	62.5	Colorless/pink	Bacterial growth
	31.25	Colorless/pink	Bacterial growth
	15.625	Colorless/pink	Bacterial growth
	7.81	Colorless/pink	Bacterial growth
	3.906	Colorless/pink	Bacterial growth
	1.95	Colorless/pink	Bacterial growth
	0.97	Colorless/pink	Bacterial growth
Group B: ZnO/Ag nanocomposite synthesized by the green method using green husk extract	500	Purple/blue	No bacterial growth
	250	Purple/blue	No bacterial growth
	125	Purple/blue	No bacterial growth
	62.5	Colorless/pink	Bacterial growth
	31.25	Colorless/pink	Bacterial growth
	15.625	Colorless/pink	Bacterial growth
	7.81	Colorless/pink	Bacterial growth
	3.906	Colorless/pink	Bacterial growth
	1.95	Colorless/pink	Bacterial growth
	0.97	Colorless/pink	Bacterial growth
Group C: ZnO/Ag nanocomposite alone	500	Purple/blue	No bacterial growth
	250	Purple/blue	No bacterial growth
	125	Purple/blue	No bacterial growth
	62.5	Purple/blue	No bacterial growth
	31.25	Purple/blue	Bacterial growth
	15.625	Colorless/pink	Bacterial growth
	7.81	Colorless/pink	Bacterial growth
	3.906	Colorless/pink	Bacterial growth
	1.95	Colorless/pink	Bacterial growth
	0.97	Colorless/pink	Bacterial growth

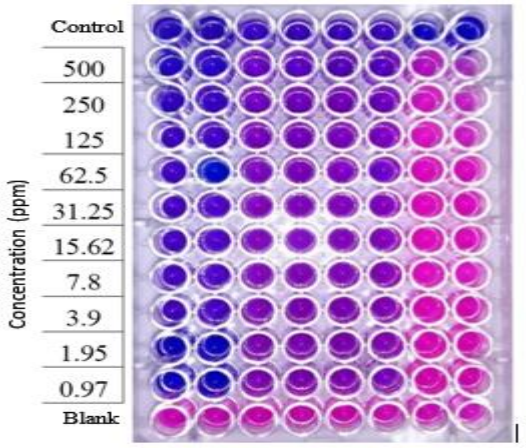

Figure 9. MIC test results in 10 studied dilutions (PPM) versus control (Chlorhexidine at a concentration of 2 mg/ml) and blank (Distilled water) concentrations

Wells and maximum optical density belonged to the positive control wells. As shown in Tables 4 and 5, the cytotoxicity decreased by decreasing the concentration in groups A (from 28% to less than 1%) and B (from 94% to less than 1%). The percentage of cell viability for group A was 73% at maximum and 99% at minimum concentration; these values were 11% and 99%, respectively for group B. As shown in Table 6, the cytotoxicity in group C decreased by decreasing the concentration (from 56% to 8%). The percentage of cell viability in group C was 41% in maximum and 96% in minimum concentration. Based on MIC test results, the cytotoxicity at 31.25 ppm was 4%.

The IC_{50} was found to be 1653 mg/ml for group A, 129.74 mg/ml for extract B, and 732.27 mg/ml for extract C. As shown, extract B was the most toxic and extract C was the least toxic extract. Two-way ANOVA with Tukey's post-hoc test revealed significant differences in the optical density of the three extracts ($p<0.001$).

Table 4. Optical density of Hela cell suspension in the presence of different concentrations of green husk hydroalcoholic extract (group A) at 540 nm.

		Concentration (PPM)								
Dilution Repetition	**Control**	**3.906**	**7.81**	**15.625**	**31.25**	**62.5**	**125**	**250**	**500**	**Blank**
1	0.89	0.68	0.80	0.82	0.80	0.86	0.89	0.89	0.86	0.03
2	0.87	0.62	0.80	0.81	0.81	0.80	0.81	0.86	0.89	0.094
3	0.89	0.62	0.80	0.83	0.86	0.86	0.87	0.82	0.88	0.03
Mean	0.855	0.647	0.80	0.824	0.826	0.845	0.861	0.863	0.884	0.051
Cytotoxicity (%)	0	28	9	7	7	4	2	2	0.001	
Viability (%)	100	73	91	93.1	93.25	95.48	97.3	97.45	99.89	

Table 5. Optical density of Hela cell suspension in the presence of different concentrations of ZnO/Ag nanocomposite synthesized by the green method using the green husk hydroalcoholic extract (group B) at 540 nm.

		Concentration (PPM)								
Dilution Repetition	**Control**	**3.906**	**7.81**	**15.625**	**31.25**	**62.5**	**125**	**250**	**500**	**Blank**
1	0.89	0.09	0.15	0.69	0.70	0.88	0.88	0.87	0.88	0.03
2	0.87	0.11	0.15	0.69	0.75	0.82	0.83	0.89	0.59	0.094
3	0.89	0.08	0.14	0.64	0.75	0.83	0.89	0.86	0.57	0.03
Mean	0.885	0.098	0.152	0.680	0.73	0.84	0.86	0.87	0.88	0.051
Cytotoxicity (%)	0	94	87	24	17	4.6	1.9	0.09	0.03	
Viability (%)	100	11	17	76	83	95	98	99	99	

Table 6. Optical density of Hela cell suspension in presence of different concentrations of ZnO/Ag nanocomposite (group C) at 540 nm.

		Concentration (PPM)								
Dilution Repetition	**Control**	**3.906**	**7.81**	**15.625**	**31.25**	**62.5**	**125**	**250**	**500**	**Blank**
1	0.58	0.29	0.38	0.52	0.59	0.58	0.50	0.51	0.53	0.03
2	0.59	0.26	0.43	0.54	0.57	0.56	0.56	0.56	0.54	0.004
3	0.59	0.24	0.44	0.52	0.50	0.56	0.58	0.57	0.55	0.03
Mean	0.592	0.27	0.424	0.531	0.55	0.568	0.55	0.55	0.544	0.021
Cytotoxicity (%)	0	66	63	53	20	18	17	16	15	
Viability (%)	100	41.7	44.3	54.2	89.2	91.2	92.1	92.8	94.4	

Discussion

This study described green synthesis and characterization of ZnO/Ag nanocomposite using the green husk extract. The cytotoxicity and antimicrobial activity of the synthesized nanocomposite against *S. mutans* were also evaluated *in vitro*. To determine the MIC and MBC of the synthesized nanocomposite against *S. mutans*, the test was repeated for 10 different concentrations of the materials. The results showed that the hydroethanolic extract of green husk at 500 ppm

concentration had no bactericidal or inhibitory effect on *S. mutans*. This test was repeated with 5000 ppm concentration which yielded the same result, and the extract had no bactericidal or inhibitory effect on *S. mutans*. The addition of ZnO nanoparticles enhanced the inhibitory effect of the extract such that it inhibited bacterial proliferation at 125 ppm concentration. The synthesized nanocomposite yielded an MIC of 31.25 ppm. A definite conclusion cannot be drawn regarding the MBC of the nanocomposite; however, the MIC in groups B and C caused a 3-log reduction in bacterial count, which is an acceptable efficacy for an antibacterial agent (Nakonieczna 2017). The MTT assay revealed that the green husk extract alone was the least toxic while ZnO nanoparticles plus the extract were the most toxic at 500 and 250 ppm concentrations compared to other concentratoin; however, at 125 ppm concentrations, over 76% of the Hela cells remained viable. Sharafatichaleshtori et al. (Sharafatichaleshtori et al. 2010) evaluated the antimicrobial activity of the ethanolic extract of walnut leaves (*Juglans regia L.*) against *Propionibacterium acnes in vitro* and reported MIC and MBC values of 12.5 and 15 mg/ml, respectively. Their results confirmed the inhibitory effect of this extract on *Propionibacterium acnes*. In the present study, the hydroethanolic extract of green husk had no significant effect on *S. mutans*.

In the current study, ZnO/Ag synthesized by the green method using the green husk extract was not more effective than the nanocomposite alone against *S. mutans*. Coating ZnO nanoparticles with silver and plant extract probably decreases the compounds such as polyphenols and flavonoids. This reduction is probably responsible for decreased antibacterial activity; this finding is in agreement with the results of Suresh et al. (Suresh et al. 2015). They showed that coating ZnO nanoparticles with *Cassia fistula* extract decreased the antibacterial compounds such as polyphenols and flavonoids. Izadiyan et al. (Izadiyan et al. 2020) evaluated the cytotoxicity of iron oxide nanoparticles synthesized by the green method using the green husk extract and showed that using this extract helped to control the size of particles.

The present study was a preliminary study to introduce an antimicrobial agent with optimal inhibitory effect on *S. mutans* and low cytotoxicity. Since this product was intended for use in children and adolescents at high risk of caries, the minimum concentration of extract (5 mg/ml) was used in this study. The results showed that 73% of the cells remained viable. In the presence of 125 ppm (MIC) concentration of nanocomposite with the green husk extract, over 76% of the cells remained viable, while over 95% of the cells remained viable in the synthesized nanocomposite group. A study on the cytotoxicity of CHX showed that CHX at 0.06% concentration caused the death of over 80% of epithelial cells after 24 hr of exposure, which was higher compared with the cytotoxicity of nanocomposite alone and in the presence of green husk extract in the current study. In the present study, over 20% of Hela cells remained viable after exposure in all study groups except for the nanocomposite group at 250 and 500 ppm concentrations, which was similar to the abovementioned study (Wyganowska-Swiatkowska et al. 2016).

Green synthesis of ZnO/Ag nanocomposite was a strength of this study. In this technique, plant extracts are used as stabilizers to decrease the size of nanoparticles and subsequently, increase their antimicrobial activity. Also, the stabilizer decreases the reaction temperature, is safe, and enhances the production of nanoparticles.

Future studies are required to assess the antibacterial effect of this extract on Gram-negative bacteria responsible for periodontal disease. Also, *in vivo* studies are required to ensure the safety of this

extract and nanocomposite for clinical use in oral health products.

Although ZnO/Ag nanocomposite synthesized by the green method using the green husk extract and synthesized ZnO/Ag nanocomposite showed lower antibacterial activity than CHX against *S. mutans*, their cytotoxicity was also lower and they significantly decreased the colony count.

Conflicts of interest

The authors have declared that there is no conflict of interest.

Ethical Considerations:

The study was approved by the ethics committee of Mashhad University of Medical Sciences (IR.MUMS.DENTISTRY.REC.1399.011).

Code of Ethics:

IR.MUMS.DENTISTRY.REC.1399.011

Authors' Contributions

Conceptualization, Supervision, and Methodology: H N and T M; Data collection, investigation and writing – original draft: A C and S H; Data analysis: H R, H F, and M D; Study design: H N; Review & editing: H N, T M, M D, H R, H F, and AC; Experimental consultation: H N and T M- Performing the experiment: M D and H R.

References

AbdElRahman HF, Skaug N, Francis GW (2002) ISSN (Print) 1013-9052 EISSN 1658-3558 Saudi Dent J 14(1):26-32

Ameh SJ, Obodozie OO, Abubakar MS, Garba M (2010) Current phytotherapy–an inter-regional perspective on policy, research and development of herbal medicine. J Med Plants Res 4(15):1508-1516

Azizi A, Fatholahzadeh B, Maleknejad P, Shamspour A, Lavaf S (2008) The effect of chlorhexidine for 12 percent of the normal oral streptococci pathogenic Microflora. J Dent (Shiraz) 9(3):299-303

Azizi S, Mohamad R, Rahim R, et al. (2016) ZnO-Ag core shell nanocomposite formed by green method using essential oil of wild ginger and their bactericidal and cytotoxic effects. Appl Surf Sci 384:517-524

Balagopal S, Arjunkumar R (2013) Chlorhexidine: the gold standard antiplaque agent. Natl J Physiol Pharm Pharmacol 5(12):270

Bandow J, Brotz H, Leichert L, Labischinski H, Hecker M (2003) Proteomic approach to understanding antibiotic action. Antimicrob Agents Chemother 47(3):948-55

Ghazal S, Akbari A, Hosseini HA, et al. (2020) Biosynthesis of silver-doped nickel oxide nanoparticles and evaluation of their photocatalytic and cytotoxicity properties. Applied Physics A 126:1-8

Ghazal S, Khandannasab N, Hosseini HA, Sabouri Z, Rangrazi A, Darroudi M (2021) Green synthesis of copper-doped nickel oxide nanoparticles using okra plant extract for the evaluation of their cytotoxicity and photocatalytic properties. Ceram Int 47(19):27165-27176

Golfeshan F, Ajami S, Khalvandi Y, Mosaddad SA, Nematollahi H (2020) The analysis of the differences between the influence of herbal mouthwashes and the chlorhexidine mouthwash on the physical characteristics of orthodontic acrylic resin. Boll Soc Ital Biol Sper 93(1)

Holister P, Weener J, Roman C, Harper T (2003) Nanoparticles. Technology white papers 3:1-11

Hosseini A, Mollazadeh H, Amiri M, Sadeghnia H, Ghorbani A (2017) Effects of a standardized extract of Rheum turkestanicum Janischew root on diabetic changes in the kidney, liver and heart of streptozotocin-induced diabetic rats. Biomed Pharmacother 86:605-611 doi:10.1016/j.biopha.2016.12.059

Iskandar B, Lukman A, Syaputra S, Al-Abrori UN, Surboyo MD, Lee C-K (2022) Formulation, characteristics and anti-bacterial effects of Euphorbia hirta L. mouthwash. J Taibah Univ Med Sci 17(2):271-282

Izadiyan Z, Shameli K, Miyake M, et al. (2020) Cytotoxicity assay of plant-mediated synthesized iron oxide nanoparticles using Juglans regia green husk extract. Arab J Chem 13(1):2011-2023

Jahanban-Esfahlan A, Davaran S, Moosavi-Movahedi A, Dastmalchi S (2017) Investigating the interaction of juglone (5-hydroxy-1, 4-naphthoquinone) with serum albumins using spectroscopic and in silico

methods. Journal of the Iranian Chemical Society 14(7):1527-1540

Jaimand K, Baghai P, Rezaee M, Sajadipoor S, Nasrabadi M (2004) Extraction and Identification of Juglone from Leaves and fresh peels of juglans regia L. by High-Performance liquid Chromatography. Iranian Journal of Medicinal and Aromatic Plants Research 20(3):323-331

James P, Worthington HV, Parnell C, et al. (2017) Chlorhexidine mouthrinse as an adjunctive treatment for gingival health. Cochrane Database Syst Rev 3(3):Cd008676 doi:10.1002/14651858.CD008676.pub2

Khattak P, Khalil TF, Bibi S, et al. (2022) Juglans Regia (Walnut Tree) Bark in Dentistry: Walnut Tree Bark in Dentistry. Pakistan Biomedical Journal 5(2):152-156 doi:10.54393/pbmj.v5i2.201

Li Y, Tanner A (2015) Effect of Antimicrobial Interventions on the Oral Microbiota Associated with Early Childhood Caries. Pediatr Dent 37(3):226-44

Lu Z, Gao J, He Q, et al. (2017) Enhanced antibacterial and wound healing activities of microporous chitosan-Ag/ZnO composite dressing. Carbohydr Polym 156:460-469 doi:10.1016/j.carbpol.2016.09.051

Maleki P, Nemati F, Gholoobi A, Hashemzadeh A, Sabouri Z, Darroudi M (2021) Green facile synthesis of silver-doped cerium oxide nanoparticles and investigation of their cytotoxicity and antibacterial activity. Inorg Chem Commun 131:108762

Mazzari AL, Prieto JM (2014) Herbal medicines in Brazil: pharmacokinetic profile and potential herb-drug interactions. Front Pharmacol 5:162 doi:10.3389/fphar.2014.00162

Mishra N, Dubey A, Mishra R, Barik N (2010) Study on antioxidant activity of common dry fruits. Food Chem Toxicol 48(12):3316-20 doi:10.1016/j.fct.2010.08.029

Moosavi Dolatabadi K, Dehghan G, Hosseini S, Jahanban Esfahlan A (2015) Effect of five year storage on total phenolic content and antioxidant capacity of almond (Amygdalus communisL.) hull and shell from different genotypes. Avicenna J Phytomed 5(1):26-33

Mozaffari B, Mansouri S, Rajabalian S, Alimardani A, Mohammadi M (2005) In vitro study between antibacterial and cytotoxic effects of chlorhexidine and persica mouthrinses. Journal of Dental School 23(3):494-509

Nakonieczna J (2017) Comment on "Effectiveness of antimicrobial photodynamic therapy (AmPDT) on Staphylococcus aureus using phenothiazinecompound with red laser". Lasers Med Sci 32(7):1667-1668 doi:10.1007/s10103-016-2107-4

Oliveira SG, de Moura FR, Demarco FF, Nascente Pda S, Pino FA, Lund RG (2012) An ethnomedicinal survey on phytotherapy with professionals and patients from Basic Care Units in the Brazilian Unified Health System. J Ethnopharmacol 140(2):428-37 doi:10.1016/j.jep.2012.01.054

Pandiyan I, Rathinavelu PK, Arumugham MI, Srisakthi D, Balasubramaniam A (2022) Efficacy of Chitosan and Chlorhexidine Mouthwash on Dental Plaque and Gingival Inflammation: A Systematic Review. Cureus 14(3)

Philip N, Leishman S, Bandara H, Walsh L (2019) Polyphenol-Rich Cranberry Extracts Modulate Virulence of Streptococcus mutans-Candida albicans Biofilms Implicated in the Pathogenesis of Early Childhood Caries. Pediatr Dent 41(1):56-62

Polizzi E, TetÃ G, Bova F, et al. (2020) Antibacterial properties and side effects of chlorhexidine-based mouthwashes. A prospective, randomized clinical study. Journal of Osseointegration 12(1):2-7

Poppolo Deus F, Ouanounou A (2022) Chlorhexidine in Dentistry: Pharmacology, Uses, and Adverse Effects. Int Dent J 72(3):269-277 doi:10.1016/j.identj.2022.01.005

Rajendiran M, Trivedi HM, Chen D, Gajendrareddy P, Chen L (2021) Recent Development of Active Ingredients in Mouthwashes and Toothpastes for Periodontal Diseases. Molecules 26(7) doi:10.3390/molecules26072001

Safarian S, Azarmi Y, Jahanban-Esfahlan A, Jahanban-Esfahlan H (2016) The beneficial effects of almond (Prunus amygdalus Batsch) hull on serum lipid profile and antioxidant capacity in male rats. Turk J Med Sci 46(4):1223-32 doi:10.3906/sag-1504-127

Sharafatichaleshtori R, Sharafatichaleshtori F, Sharafatichaleshtori A, Rafieian M (2010) Antibacterial effects of ethanolic extract of walnut leaves (Juglans regia) on propionibacterium acnes. Journal of Advances in Medical and Biomedical Research 18(71):42-49

Suresh U, Murugan K, Benelli G, et al. (2015) Tackling the growing threat of dengue: Phyllanthus niruri-mediated synthesis of silver nanoparticles and their mosquitocidal properties against the dengue vector Aedes aegypti (Diptera: Culicidae). Parasitol Res 114(4):1551-62 doi:10.1007/s00436-015-4339-9

Wang S, Wu J, Yang H, Liu X, Huang Q, Lu Z (2017) Antibacterial activity and mechanism of Ag/ZnO nanocomposite against anaerobic oral pathogen Streptococcus mutans. J Mater Sci Mater Med 28(1):23 doi:10.1007/s10856-016-5837-8

Waqar SM, Huma A, Razi A, Saher F, Qureshi SS, Qureshi JA (2022) Formulation Development and Evaluation of Propolis Mouthwash for Treatment of Periodontal Disease. Journal of Xi'an Shiyou University (Natural Science Edition) 18(10):342-357

Wyganowska-Swiatkowska M, Kotwicka M, Urbaniak P, Nowak A, Skrzypczak-Jankun E, Jankun J (2016) Clinical implications of the growth-suppressive effects of chlorhexidine at low and high concentrations on human gingival fibroblasts and changes in morphology. Int J Mol Med 37(6):1594-600 doi:10.3892/ijmm.2016.2550